Square-core bundles for astronomical imaging

Julia J. Bryant[a,c] & Joss Bland-Hawthorn[a,b]

[a] Sydney Institute for Astronomy (SIfA), School of Physics, The University of Sydney, NSW, Australia 2006;
[b] Institute of Photonics & Optical Science, The University of Sydney, NSW, Australia 2006;
[c] ARC Centre of Excellence for All-sky Astrophysics (CAASTRO).

ABSTRACT

Optical fibre imaging bundles (hexabundles) are proving to be the next logical step for large galaxy surveys as they offer spatially-resolved spectroscopy of galaxies and can be used with conventional fibre positioners. Hexabundles have been effectively demonstrated in the Sydney-AAO Multi-object IFS (SAMI) instrument at the Anglo-Australian Telescope[5]. Based on the success of hexabundles that have circular cores, we have characterised a bundle made instead from square-core fibres. Square cores naturally pack more evenly, which reduces the interstitial holes and can increase the covering, or filling fraction. Furthermore the regular packing simplifies the process of combining and dithering the final images. We discuss the relative issues of filling fraction, focal ratio degradation (FRD), and cross-talk, and find that square-core bundles perform well enough to warrant further development as a format for imaging fibre bundles.

Keywords: Square-core optical fibre; hexabundles; astronomical instrumentation

1. INTRODUCTION

Imaging fibre bundles are the future of multi-object spectroscopy as they allow spatially-resolved imaging of many galaxies across a field. This technology is the next logical improvement on multi-object spectroscopy that has traditionally been done with single fibres. Fused imaging fibre bundles, or 'hexabundles'[1,2,3] have been developed using circular-core fibres and are now operational in a multi-object IFU on the Anglo-Australian Telescope (AAT), called SAMI[5]. The advantage of hexabundles is that the circular cores are tightly pack in order to increase the filling fraction (ratio of *area of cores* to *total bundle area*), however they are not in a rigorously symmetric grid pattern. This poses a problem when galaxy images are dithered and need to be recombined. Since observations are always background limited in galaxy surveys (at least up to $R \sim 5000$), dithering is required to remove the bundle footprint. Fogarty et al. (2012) discusses the complexities of recombining images, particularly when dithered, if the fibres are in an irregular pattern. A disadvantage of combined data of this form is a variable signal-to-noise ratio across the field.

Post-processing would be simpler if the fibres were in a regular grid pattern within the hexabundle. The two most regular patterns of fibres to consider are a rigorously hexagonal grid of circular fibres, or square cores evenly-packed. Both of these would simplify the recombination of dithered images. However, fusing a regular hexagonal fibre array is difficult. Square-core fibres naturally pack evenly and can result in smaller, regular interstitial holes. The filling fraction can then be higher, with the advantage of an even grid. Therefore we aim to investigate the effect of square cores on the optical performance and consider the trade-off with filling fraction and image reconstruction.

Previous papers have tested square-core fibres with a view to their potential properties for scrambling modes along the fibre. This can lead to a more stable and uniform energy distribution on output. The application of modal scrambling is relevant to single fibres but not so much to fibre bundles in which the core diameter is matched to the seeing disk. However, results from those papers have been inconclusive with regard to FRD from square-core fibres. Chazelas et al. (2010) found promising FRD results in square-core fibres but unexplained structures were seen in the far field images that were potentially linked to alignment issues in the test apparatus. However, a report by Feger, Goodwin & Poppett (2011) demonstrated that a $200 \times 200\mu$m core square fibre has

J.J.B.: E-mail: jbryant@physics.usyd.edu.au

worse FRD than other fibres shapes, with half the core diameter. The effect of core diameter was not decoupled from the impact of fibre shape on FRD.

In the current tests we have used an FRD testing apparatus that has been well characterised through tests of circular-core single fibres and hexabundles. While all FRD tests can introduce some FRD from the test-setup itself, the comparative performance between square and circular-core fibres will tell us how successful the square cores fibres could be compared to the current circular-core bundles and bare fibres.

1.1 Filling fraction

One key advantage of an evenly packed square-core bundle is the potential increase in filling fraction. Figure 1 shows the relationship between cladding thickness and filling fraction for square-core bundles compared to those formed from a uniformly packed hexagonal array of circular cores. The filling fraction in the latter case is assumed to be within a hexagonal outer region just containing the cores. Therefore the outer edge of the bundle will have losses that have a less significant impact on filling fraction when there are a larger number of cores. If the edges of the bundle are disregarded, the filling fraction is that of an infinite array of cores. Hexabundles made from fused circular fibres that are not strictly hexagonally packed (as used in SAMI, and shown in Figure 2 below) have a filling fraction that depends on the level of fusing and the fibre packing. The median value for the SAMI cores is 0.72. While hexagonal packing should give a higher filling fraction than the irregular packing, the fusing process decreases the cladding thickness slightly at contact points between cores, which in turn boosts filling fraction. A fused hexagonal array could therefore have slightly higher filling fractions than the theoretical values shown on the plot.

For a 100μm-core fibre, square-cores clearly give a larger filling fraction than either the fused circular core hexabundle or the hexagonally-packed circular core bundles. This is the case for all cladding thicknesses above 3μm, within the range shown, that gives acceptable cross-talk in a fused bundle[2]. The trade-offs between filling fraction and cross-talk for the square-core bundles are discussed in Section 4.2.

2. 25-CORE SQUARE FIBRE BUNDLE

We have tested a commercial square-core fibre bundle shown in Figure 2 (left). It was manufactured by CERAMOPTEC, using Optran WF195X195A fibre with a $195 \times 195\mu$m core and $227 \times 227\mu$m cladding with acrylate coating which is removed at the bundle end. The NA of the fibre is 0.22. 25 pieces of fibre were arranged in a square and mounted in an SMA connector and the end face was polished. The cores are not strictly square. Due to manufacturing limitations, the corners are slightly rounded. The CERAMOPTEC fibres have a ratio of corner curvature radius to fibre core width of 0.08 ± 0.02, where the error comes from measuring the curvature from a microscope image of the bundle face - the fibre-to-fibre radius is much more consistent.

Unlike our SAMI circular-core hexabundles (Figure 2 right), the square-core bundle is not fused. If square cores were to be used for astronomical applications, fused bundles would be made with more even packing and reduced cladding to ensure a larger filling fraction. The filling fraction of this square bundle is quite low, but serves to test the fibre properties when bundled. Increasing the filling fraction by decreasing the cladding thickness will also increase the cross-talk between cores (light leaking from one core to adjacent cores). While the packing in the CERAMOPTEC bundle is not strictly uniform due to their manufacturing limitations, the closest pack cores can be used to set limits on the cross-talk for this cladding thickness.

We also tested $200 \times 200\mu$m core bare square fibre, the same fibre used in the bundles. These were compared with the performance of smaller cores in the same fibre type (WF100 $\times$ 100/123 $\times$ 123μm core/cladding) and circular-core 105/125μm bare fibre used in the SAMI hexabundles.

3. EXPERIMENT METHOD AND DATA REDUCTION

The square-core bundle was tested for cross-talk and focal ratio degradation (FRD). The test set-up consisted of an Oriel LED light source which was fed through a filter holder in which a Bessel B-band or Bessel R-band filter was placed in turn. The combination of the LED transmission function and that of the Bessel filters gave a peak wavelength in the blue filter, at 457 nm and FWHM of 27 nm, while the red was centred on $\sim$ 596nm

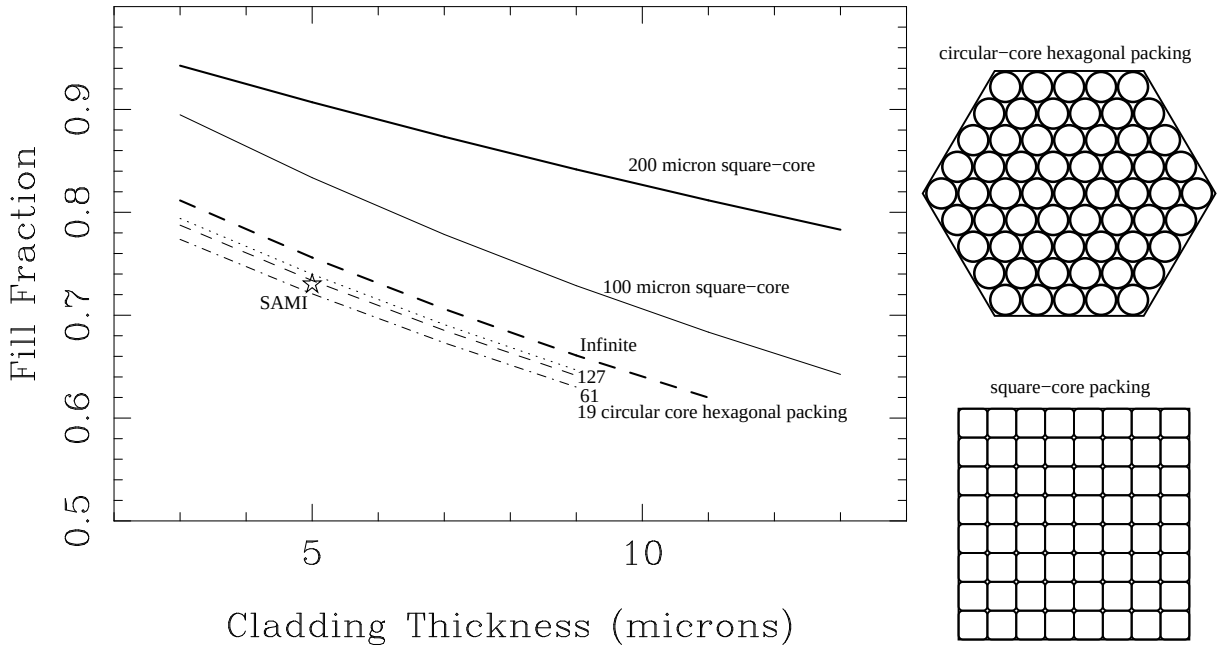

Figure 1. The filling fraction (ratio of core area to total bundle area) is shown for a range of cladding thicknesses. A higher filling fraction means that less light is lost between cores and in interstitial holes. The solid lines are for a perfectly even grid of square-core fibres (as shown bottom right) with $105 \times 105\mu$m (thin line) and $200 \times 200\mu$m (thick line) core diameters. In reality the square cores have slightly rounded corners, and the effect of this is to decrease the filling fraction by less than 1%. A perfect hexagonal array (illustrated top right) of 105μm-diameter circular cores is shown for different numbers of cores (19 core - dot-dash; 61 cores - dashed; 127 cores - dotted). The hexagonal array filling fraction includes the edge effect due to the lost space within a hexagonal bundle, however, the thick dashed line shows the maximum filling fraction for a regular packed hexagonal array with no edge effects (or an infinite number of cores). The star marks the median filling fraction of the current SAMI instrument hexabundles.

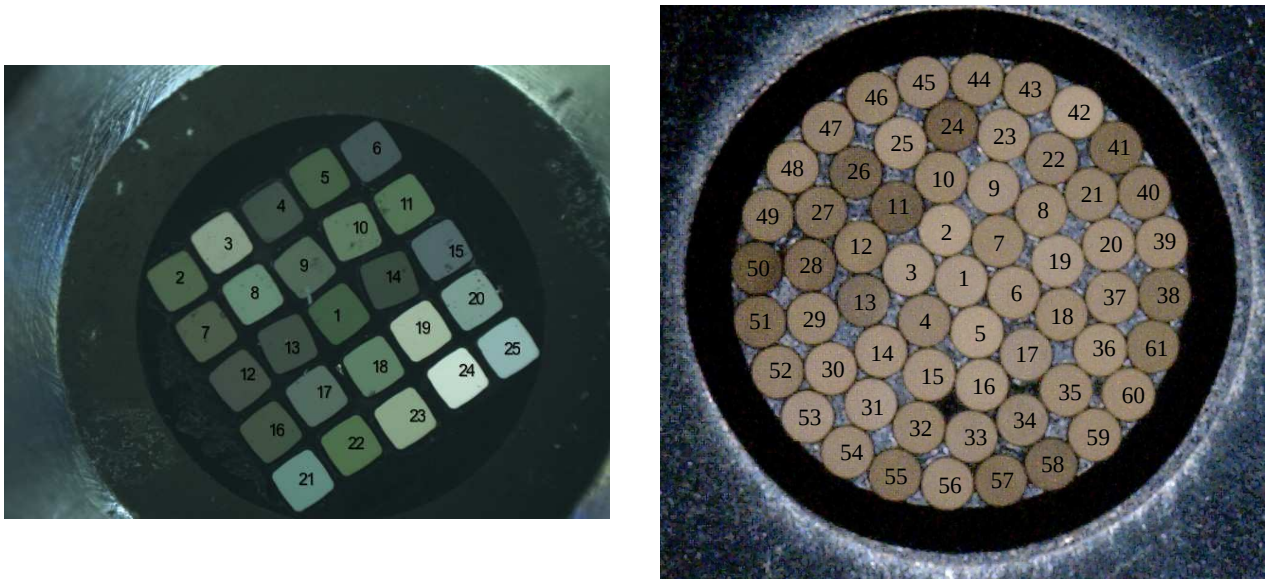

Figure 2. Left: The square-core bundle tested in this paper. Each of the 25 fibres have $195 \times 195\mu$m cores. The fibres are separate on output and only bundled for the first few centimetres. Right: One of the 61-core fused hexabundles used in the SAMI instrument. The cores are 105μm in diameter.

with an asymmetric profile of FWHM 60 nm. This light was focussed into a multi-mode fibre which was then re-imaged through an aperture (to set the input NA) and focussed onto the bundle or fibre being tested. The resultant focussed spot was $< 50\mu$m by zero intensity. Back focus input images were recorded by translating the camera a precise distance behind the focus. From this data, the input NA for each aperture size was confirmed for both the blue and red filters.

The output of the fibre being tested was cleaved and mounted on a V-groove plate that was aligned to a pair of large camera lenses. The fibre was therefore re-imaged onto an SBIG camera with 5μm pixels. A micrometer stage allowed the camera to be shifted to a specific back-focus position.

3.1 Errors due to alignment of the optics and positioning of the fibres

Small misalignments in the optical test setup can contribute to the measured FRD. Therefore careful analysis of all contributions to errors were assessed.

3.1.1 Input into the hexabundle

The NA input into the hexabundle was measured using a camera in place of the hexabundles holder. Any angle between the camera and the input beam will record an incorrect input NA. The error in the input NA measurements due to the alignment of the camera to the input beam is ± 0.0005. Positioning the fibre holder relative to the input beam introduces an error in NA into the fibre of $< \pm 0.001$. Repositioning error for the input aperture gives an NA error of $< \pm 0.0005$. The bare fibre was tested by mounting the input end into a bare fibre adaptor. The pressure of the bare fibre adaptor introduces a small amount of FRD. For input F/3.5, the FRD is much smaller than the errors given here, however by F/5.8 the output NA at 90% encircled energy can be increased by as much as 0.01.

3.1.2 Output images

The V-groove plate was aligned with the optical axis, however, there are slight angle differences depending on each fibre. This is due to *both* how the fibres sit in the V-grooves and potentially any differences in the cleaves. These errors were measured by shifting the V-groove plate back and forward and imaging the shift in each core. These shifts contribute directly to the FRD measurements and gave an NA error of up to ± 0.004. Alignment of the camera was found to give an NA error $< \pm 0.001$. The focussing of the output fibre introduces an error because it is very difficult to get an exact focus on a multimode fibre. We could focus at best to ± 0.02 mm, which gives an error in NA of $\pm 0.0133 \times$NA, or ± 0.0013 and ± 0.003 for an output NA of 0.1 and 0.2 respectively. The fibres were cleaved on the output end, and the effect of the cleave on the FRD results was quantified with repeated cleaves using several different cleavers. Each cleave was checked under a microscope to ensure the edge crack did not penetrate the core and that the cleave was straight to within $<<$ 1 degree. The variation between such cleaves gave a maximum variation in output NA (at 90% encircled energy) of ± 0.002.

All errors were combined in quadrature to give the measurement error, and then the small profile fitting errors were included to give the total errors shown on the plots. Time variation in the input light intensity plus variations in the SBIG camera response, were quantified with repeated images through one core of the bundle of time periods ranging from second to hours. The maximum variation in resulting integrated counts was $< 1.0\%$ with typical values of $\sim 0.2\%$.

3.2 Measurement of fibre cross-talk and FRD

Several cores in the square-core bundle and the several single bare fibres were tested in turn. The input light was centred on the core, and images were taken with the SBIG camera for focal ratios of F/3.5 to F/6 (input NAs of 0.14 to 0.084) through both filters. Cross-talk from the bundle core that had the injected light, into adjacent cores was measured by imaging the surrounding cores. FITS images from the SBIG camera were processed using the IRAF astronomical data reduction software[9]. Firstly each image was dark subtracted. Then the barycentre of the fibre image was fit, and the total integrated counts were measured by selecting a fixed aperture size for all fibres that was large enough to include all the output from the fibre.

Focal ratio degradation (FRD) causes the opening angle of the output beam to be larger than that of the input beam. The encircled energy was measured from images in the far field at a precise back-focus distance.

Aperture photometry in IRAF gave the encircled energy as a function of radial pixels. Using the known pixel size of the camera, an NA value was calculated from $\sin\theta$ of the cone angle. This gives the effective output NA at each point across the image of the fibre. The resulting plots of NA vs encircled energy will therefore be shifted to the right for a larger output cone angle, indicating worse FRD.

4. RESULTS

4.1 Focal Ratio Degradation (FRD)

The encircled energy profile of a selection of fibres in the bundle was measured against the output NA. Figure 3 shows the encircled energy profiles through both the Bessell blue (0.46μm) and red (0.60μm) filters. The profiles through the red filter are at a lower NA than those through the blue filter because the shorter wavelengths have more modes and therefore a higher NA. It is well known that FRD is worse (curves are shifted further to the right compared to the input encircled energy profile) for larger input F/#s (e.g. [2],[8]) and therefore we have tested a range of input F/#s. However, in astronomy, typically fibres are used for systems with F/#$<\sim 4$. The FRD is quantified for different input f-ratios in Figure 4 in terms of:

- The output encircled energy within the same F/# as was input. The larger the encircled energy, the less the output beam has spread out due to FRD.

- The output F/# when the encircled energy is at 90%. The further the curve sits below the line of equality, the worse the FRD.

- The increase in NA at output compared to that of the input light at 90% encircled energy.

The FRD in each of the square bundle cores tested, were in agreement within errors, showing a consistency in the performance of the cores. Several cleaves were taken of each core and the effect of the cleaves was included in the error measurement. We then compared the performance of the square cores in the bundle to a single $200 \times 200\mu$m fibre (WF $192\times192/218\times218\mu$m) with square cladding and core. In Figure 4 the square bundle fibres perform only a little worse than the single $200 \times 200\mu$m square core fibre at F/3-4, however, by F/6, there is a marked performance loss due to the bundling of the fibres. We have previously found that fused circular bundles can be made to perform nearly as well as single circular cores at low input F/#s and we believe that we can improve the square core bundle performance using a fused bundle.

However, in order to replace current circular-cored bundles with square cores, we would require the same FRD performance. Fibres with different core sizes will vary in their performance, due to larger cores carrying more modes, and our previous bundles have all been made with 105μm core circular fibre. In Figure 4 the 200μm core results are compared to that for both a circular and a square 100μm core fibre. We show that the latter square-core fibre has just as low FRD as the circular-core fibre of the same diameter. We plan to develop a $100 \times 100\mu$m fused square bundle which should out-perform the packed bundle tested here. As discussed above, we therefore expect that it will perform nearly as well as the $100 \times 100\mu$m single square core fibre and this would result in comparable FRD to circular fused bundles. This will need to be confirmed, but the comparison of the larger square-core bundle to the single fibres indicated that it is worth pursuing square-core fibre bundles for astronomical imaging.

4.2 Cross-talk and filling fraction

Cross-talk was measured for several fibres in the bundle by measuring the integrated counts in an adjacent fibre while the light was centred on the target fibre. Due to the slightly irregular packing of the cores in the CERAMOPTEC bundle, the cross-talk into adjacent cores was not equally distributed. Therefore, two pairs of cores which have the smallest separation and longest, most even contact, were selected as the most representative measures of expected cross-talk in an evenly packed bundle. In Figure 2 these pairs are marked as cores 2/7 and 18/23.

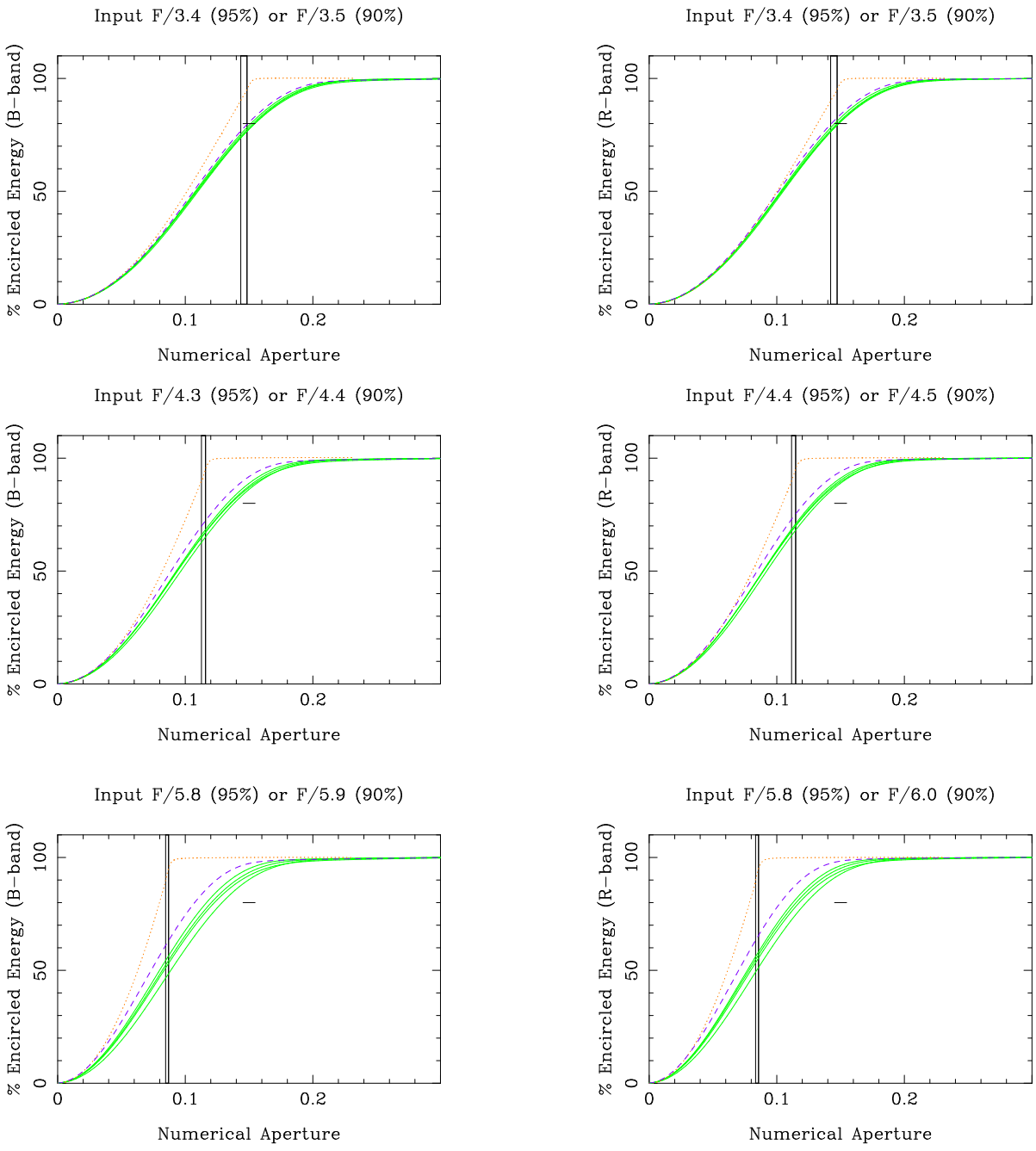

Figure 3. *Encircled energy vs output numerical aperture (NA)* The light profile input into the fibres is shown by the dotted orange line. Solid green lines show the results for a selection of cores within the square-core bundles, while the dashed purple line is a single fibre of the same type. Several different input focal ratios are shown as listed on the plots with the NA of those inputs marked by vertical black lines at 90% and 95% encircled energy. The plots on the left are through the blue (0.46μm) filter and those on the right are through the red (0.60μm) filter. A black horizontal line marks the typical error bar when NA=0.15.

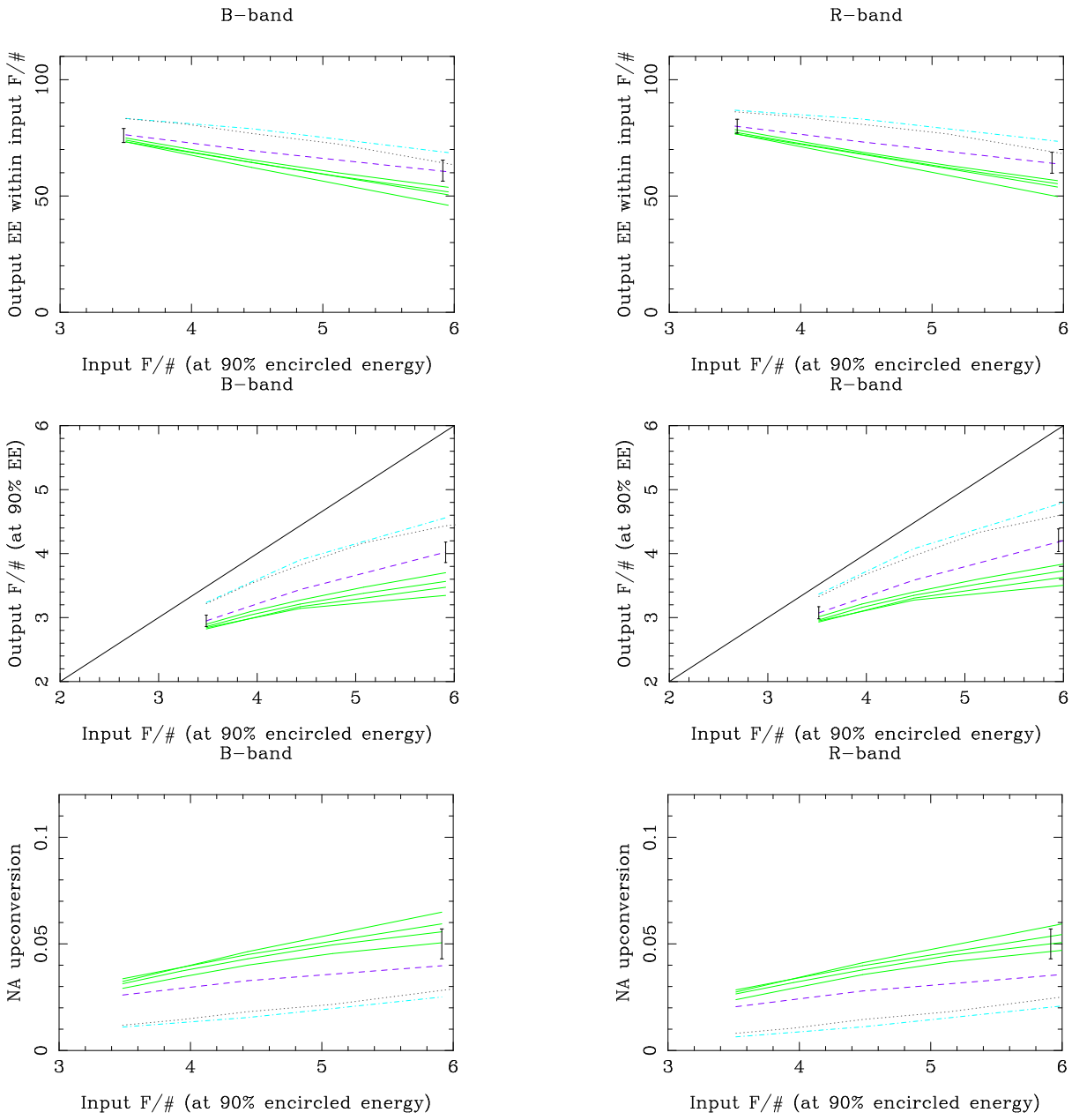

Figure 4. *FRD results.* Input focal ratio vs the encircled energy within the same focal ratio on output (top), output focal ratio (middle), NA up-conversion (lower). Solid green lines show the results for a selection of cores within the square-core bundles, while the dashed purple line is a single fibre of the same type. Results for single 100μm core circular (grey dotted) and square fibres (cyan, dot-dash) are also shown. The plots on the left are through the blue (0.46μm) filter and those on the right are through the red (0.60μm) filter.

The total loss into adjacent fibres was assumed to be 4 times the loss into one adjacent fibre, for a regular geometry. This total cross-talk was found to be $0.1 - 0.12 \pm 0.02\%$ (0.0043-0.0052 dB loss) with the blue filter, and $0.084 - 0.11 \pm 0.02\%$ (0.0036 - 0.0048 dB loss) in the red filter, for an input F/# of 3.5 (at 90% encircled energy). The given error is due to the fitting and measurement errors, while the range indicates the variation between cores tested.

These cross-talk values in this square bundle are less than the cross-talk found between circular cores in hexabundles (see [2]). For example, hexabundles with a cladding thickness of $5-8\mu$m had cross talk of $0.4-0.2\%$ for input F/3.5. However, the cross-talk increases with the cladding thickness and also with cladding contact length. The cladding thickness of the square-core fibre used in the bundles is 16μm and is therefore much larger. However, slight misalignment of the cores due to the manufacture of the bundle, means that the actual separation of the cores was not always 32μm, and instead varied up to 47μm. Cladding thickness does not scale linearly with cross-talk[1], rather a factor of two increase in cladding thickness has been shown to give more than a factor of 5 decrease in cross-talk in a number of cases. However, this would need to be tested with square-core bundles from fibre with different square cladding thicknesses. Circular cores with such a large cladding thickness would have very much less cross-talk but the larger contact area of the square cores increases the cross-talk.

The contact area of the fibres in a square-core bundle will be ~ 3.2 times that of the fibres in the SAMI bundles, assuming that only the straight sides and not corners are in contact on the square fibres. Therefore, we may possibly expect the cross-talk to reach 1.28% (3.2 times the 0.4% found in the circular cores) for F/3.5, if the cladding is 5μm thick as in the circular-core hexabundles. However, if the FRD turns out to be worse in a $100 \times 100\mu$m square-core bundle than a circular core when measured, then the cross-talk may be higher than this.

Higher cross-talk is however, offset by the better filling fraction of the square bundles, which also depends on the cladding thickness. In order to have an equal filling fraction to the hexabundles currently in use on the SAMI instrument (73%), Figure 1 shows that the cladding thickness of a $100 \times 100\mu$m square bundle could be as high as 9μm, or 18μm core separation. However, a square bundle with 5μm cladding will have a filling fraction of 83% - very much higher than the circular-fibre bundles. Therefore a 10% increase in filling fraction may be achieved with only a couple of percent cross-talk. Cross-talk tests will be done on the next generation square-core bundle with $100 \times 100\mu$m fused cores, to confirm these cross-talk predictions. Depending on both the seeing and the scattering in the spectrograph, this level of cross-talk may not be high enough to out-weight the benefits of a larger filling fraction and even grid of cores.

Consider the effect of cross-talk compared to seeing. If the square core had a diameter equal to the FWHM of the seeing disk size, then 57.9% of the power in the seeing gaussian would fall within the central square. The grid of 8 surrounding cores (illustrated in Figure 5) would then have 42.0% of the power between them (as 0.1% lies outside those cores). The distribution of power between these 8 cores is not even as the diagonal cores will have 1.42% of the total power each, while the 4 cores that have the contact side to the central core, will each have 9.08% of the total power. Therefore the percentage of power that falls in one edge core compared to the centre core is 15.7%, and these are the cores used for the cross-talk calculation. If the cross talk was 1.28% as discussed above, then the cross-talk would be only 0.08 of the power scattered into the adjacent core by seeing and therefore, at this level the cross-talk is not significant. If the core diameter is larger than a seeing disk size, then the cross-talk will become more significant.

5. CONCLUSION

We have compared the performance of a 25-core unfused square-core bundle to that of single square-core and circular-core fibre and circular-core fused hexabundles. The square-core fibres in the bundle had only slightly worse FRD to the single bare-fibre of the same type at F/3-4, but the FRD was worse than for our existing hexabundles simply because the core diameter is double the size. The larger core size of the square fibres intrinsically has more FRD than a smaller-core square fibre, however we found that a $100 \times 100\mu$m square core single fibre has similar FRD characteristics to a 100μm core circular fibre. Therefore, we believe that with improved manufacture, our new fused $100 \times 100\mu$m-core square bundles may have just as good FRD as the current circular-core hexabundles. The cross-talk between the core was found to be negligible, as the cladding

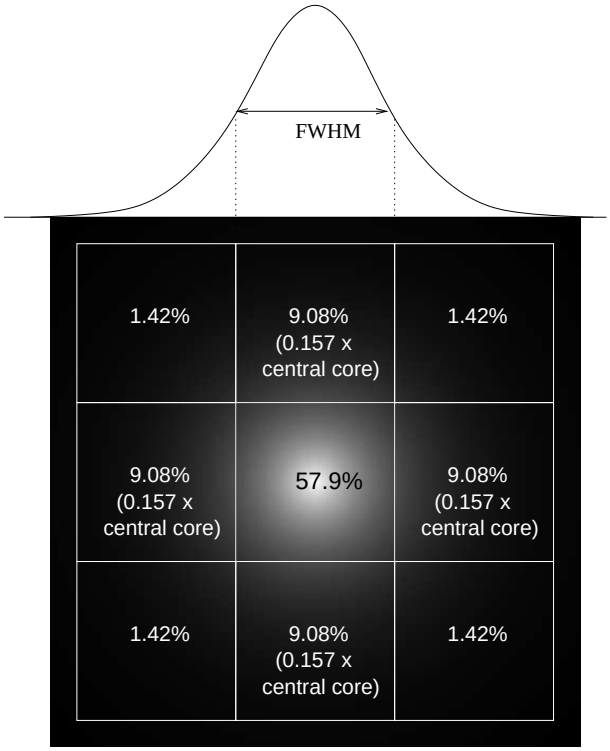

Figure 5. Percentages of the power from a seeing gaussian, in each square core of a bundle when the core diameter matches the FWHM of the seeing disk. Cross-talk of 1.28% is only 0.08 of the light already put into adjacent cores by the seeing disk profile.

thickness was large. Scaling the cross-talk based on cladding thickness and contact area, we predict a $100\times100\mu$m square core square bundle will have $\sim 1.3\%$ cross-talk at F/3.5, which is small compared to the effects of seeing, and the filling fraction of such a bundle will be 10% higher than for circular-cored hexabundles. Therefore, we conclude that square-core bundles warrant further development for astronomical applications in spatially resolved spectroscopy, as the initial tests show their optical performance may be sufficient, and they have the distinct advantage of a large filling fraction as well as an even grid of cores to simplify post-processing of images.

6. ACKNOWLEDGEMENTS

JJB is funded by the ARC Centre of Excellence for All-Sky Astrophysics (CAASTRO). This research was conducted by the Australian Research Council Centre of Excellence for All-sky Astrophysics (CAASTRO), through project number CE110001020. JBH is an ARC Federation Fellow supported by ARC grant FF00776384 which supports the Astrophotonics programme at the University of Sydney. We are extremely grateful to the extended astrophotonics group in Sydney and the staff of the Anglo-Australian Observatory for their continued interest in our quest to optimize hexabundles.

7. REFERENCES

[1] Bryant J. J., O'Byrne J. W., Bland-Hawthorn J., Leon-Saval S. G., "Characterisation of hexabundles: initial results", MNRAS 415, 2173 (2011)
[2] Bryant J. J., Fogarty L., Bland-Hawthorn J., Croom S., "Focal ratio degradation in lightly-fused hexabundles", in prep (2012)
[3] Bland-Hawthorn J. et al., "Hexabundles: imaging fiber arrays for low-light astronomical applications" , Optics Express, 19, 2649 (2011)
[4] Chazelas B., Pepe F., Wildi F., Bouchy F., Perruchot S., Avila G. , "New Scramblers for precision radial

velocity : Square and Octagonal fibers.", Proc. SPIE 7739, 773947-773947-9 (2010)
[5] Croom S., et al. "The Sydney-AAO Multi-object Integral field spectrograph (SAMI)", MNRAS 421, 872 (2012)
[6] Feger T., Goodwin M. and Poppett C.L.,"Focal Ratio Degradation study of non-circular shaped fibres", http://astrospectroscopy.files.wordpress.com/2011/06/noncircular-fibres.pdf (2011)
[7] Fogarty L. in prep (2012)
[8] Poppett C.L. & Allington-Smith J.R., "The dependence of the properties of optical fibres on length", MNRAS 404, 1349 (2010)
[9] Tody, D., "The IRAF Data Reduction and Analysis System", Proc. SPIE 627, 733 (1986)